Check for updates

Solution electrospinning and properties of poly(ethylene 2,5-furandicarboxylate) fibers

Mariia Svyntkivska [a,*], Tomasz Makowski [a], Ele L. de Boer [b], Ewa Piorkowska [a]

[a] Centre of Molecular and Macromolecular Studies Polish Academy of Sciences, Sienkiewicza 112, 90-363, Lodz, Poland
[b] Avantium Renewable Polymers BV, Zekeringstraat 29, 1014 BV, Amsterdam, the Netherlands

ARTICLE INFO

ABSTRACT

Poly(ethylene 2,5-furandicarboxylate) (PEF) is an attractive bio-based alternative to petroleum-based polymers. In this work, novel PEF-based nonwovens were obtained by the solution electrospinning, using as solvents: trifluoroacetic acid, its mixtures with dichloromethane and dichloroethane, and also 1,1,1,3,3,3-hexafluoro-2-propanol. The effect of the solvent type and PEF concentration on the fiber thickness and the properties of nonwovens was studied. The average thickness of nonwoven fibers ranged from 180 nm to 2.3 μm. The fibers were amorphous with the glass transition temperature of 85–87 °C. The nonwovens were strongly hydrophobic, with water contact angles of 144–146° although they exhibited the rose petal effect. The mechanical properties of the materials were influenced by their porosity and fiber thickness. The nonwoven electrospun from 20 wt% PEF solution in trifluoroacetic acid, with an average fiber diameter of 2.13 μm and a porosity of 74%, exhibited the highest tensile strength and elongation at break, 10.8 MPa and 190%, respectively.

1. Introduction

Poly(ethylene 2,5-furandicarboxylate) (PEF) is attracting increasing attention from both academy and industry [1–5]. Being synthesized from biomass-based 2,5-furandicarboxylic acid (FDCA) and ethylene glycol, PEF is a bio-based alternative to petroleum-based polymers, especially poly(ethylene terephthalate) (PET). FDCA is obtained by controlled oxidation of 5-hydroxymethylfurfural, which is produced by triple dehydration of C_6 sugars such as fructose or glucose, while bio-ethylene glycol can be obtained from bio-ethanol or by hydrogenolysis of sugars [2,6]. Nowadays, the development of bio-based polymers is the subject of intensive research because of their vital role in struggling with carbon dioxide emissions and in decreasing dependence on fossil resources. Moreover, being a close polyester family member of PET, PEF can be recycled in a similar way to PET using existing mechanical recycling assets. The attractive properties of PEF make it potentially useful in many applications, for instance, in bottles, films and fibers [1,3,4,7,8]. PEF is a slowly crystallizing polymer, with the melting temperature in the range of 200–230 °C [9,10] and the glass transition temperature (T_g) around 85 °C [2,9]. According to Knoop et al. [11] PEF elastic modulus at 25 °C, 2470 MPa, exceeds that of PET, 2000 MPa. PEF barrier properties to gases and liquids are better than

those of PET. The permeability of amorphous PEF to oxygen, carbon dioxide and water is 11, 19 and 2.8 times lower than that of amorphous PET [12–16]. PEF can be viewed as a PET analogue, in which the benzene ring is replaced with a furan ring. The absence of ring-flipping of the furan ring in PEF and the lower bond angle of the carboxyl groups on the furan ring, compared to the arrangement on the benzene ring, increase the energy barrier for cooperative motions to occur. This results in decreased PEF chain mobility in the amorphous state and is responsible for the higher T_g, elastic modulus and barrier properties as compared to PET [2]. The higher barrier properties of PEF are also attributed to the dipole moment of the furan ring [17].

Tuning the properties of PEF is possible by copolymerization [18–22], and by filling or blending, for instance, with nanocellulose, montmorillonite, titanium dioxide, or poly(propylene 2,5-furandicarboxylate) [23–27]. So far, most reports on the PEF studies are focused on synthesis [1,7,28], mechanical properties [29,30], crystallization [10,31,32], and barrier properties [12,14,15].

Despite the wide potential applications of PEF fibers, only a few reports were published, concerning the melt spinning of fibers of PEF, poly (ethylene terephthalate-co-ethylene 2,5-furandicarboxylate) and poly (ethylene 2,5-furandicarboxylate-co-ethylene glycol) [19,33–35]. The wet spinning of blends of polylactide with FDCA based polymers [36,37]

---

* Corresponding author.
E-mail address: mariiasv@cbmm.lodz.pl (M. Svyntkivska).

was also reported.

It must be emphasized that synthetic textiles are widely used in many applications. One of the methods of obtaining polymer fibers is electrostatic fiber formation, known as electrospinning. The fibers form during stretching and elongation of charged drops of polymer solution or melt in a strong electrostatic field during the motion of polymer jets to a collector, on which nonwoven mats are created. The advantage of producing fibers by polymer solution electrospinning is that this process does not require high temperatures. During the electrospinning, a solvent evaporates, which results in the solidification of a polymer. Morphology of the electrospun nonwovens and fiber diameters are determined by the solution characteristic and process parameters. A general trend of formation of different structures, from discrete droplets and fibers with bead-like defects to fibers with uniform diameters, and a further increase in the fiber diameters with increasing polymer concentration, were observed, due to an increase in solution viscosity and surface tension [38,39]. Numerous polymers are suitable for electrospinning, including polyamides, PET, polylactide, cellulose acetate and polyvinyl alcohol [40,41]. A wide range of electrospun fibers of different polymers with various diameters was obtained. Their modifications have been extensively studied for applications in diverse fields, for instance, air and water filtration [42–44], food packaging [45,46], tissue engineering, reconstructive medicine, and drug delivery systems [47–49].

In this work, PEF nonwovens were successfully electrospun from PEF solutions in trifluoroacetic acid, in mixtures of trifluoroacetic acid with dichloromethane and dichloroethane, and in 1,1,1,3,3,3-hexafluoro-2-propanol. A series of electrospun nonwovens containing fibers with average diameters ranging from 180 nm to 2.3 μm was obtained and examined. The water wettability, as well as the mechanical and thermal properties of the obtained nonwovens, were investigated.

2. Experimental

2.1. Materials

Poly(ethylene 2,5-furandicarboxylate) (PEF) was obtained from Avantium Renewable Polymers (the Netherlands). The PEF grade used was G90P with an intrinsic viscosity of 0.86 dL/g, as measured according to ASTM D4603, and weight average molar mass (M_w) of 128 kg/mol, as determined using gel permeation chromatography with 1,1,1,3,3,3-hexafluoro-2-propanol (HFIP) as a solvent and a classical calibration with a poly(methylene methacrylate) standard. To dissolve PEF, the following solvents were used: trifluoroacetic acid (TFA) (purity of 99.9%) from Chemat (Poland), dichloromethane (DM) (purity of 99.5%) from StanLab (Poland), dichloroethane (DE) (purity of 99.5%) from Chempur (Poland) and HFIP (purity of 99%) from Apollo Scientific (Poland).

2.2. Preparation of nonwovens

PEF granules were dried under reduced pressure (0.1 bar) for 16 h at 140 °C and then dissolved to obtain PEF solutions with different concentrations. The parameters of the electrospinning process and sample codes are shown in Table 1. The PEF nonwovens were electrospun in an environmental chamber at room temperature (RT) and controlled relative humidity of 30–35%, using a high voltage power supply CM5 Simco-Ion (the Netherlands) and static square aluminum collector, 20 cm x 20 cm. The solutions were dosed with syringes as nozzles, and the dosing rate was controlled by a stepper motor T-LLS105, Zaber Technologies (Canada). The applied voltage and the distance from the nozzle to the collector were 15 kV and 25 cm, respectively. After the electrospinning process, the nonwovens were dried for 24 h under reduced pressure (0.1 bar) at 60 °C. An increase in drying time was ineffective, hence to further reduce the residual solvent content, additional drying at 100 °C for 24 h was necessary. To prevent deformation and shrinkage during drying

Table 1
Parameters of electrospinning of PEF nonwovens.

Sample code	PEF concentration (wt %)	Solvents	Needle gauge and (inner diameter (mm))	Flow rate (mL/h)
20TFA	20	TFA	16 (1.19)	1.5
15TFA	15	TFA	18 (0.84)	1.5
12TFA	12	TFA	18 (0.84)	1.5
10TFA	10	TFA	22 (0.41)	1.0
8TFA	8	TFA	26 (0.26)	0.15
6TFA	6	TFA	26 (0.26)	0.15
12TFA/DM	12	TFA/DM (1/3 vol/vol)	18 (0.84)	1.5
12TFA/DE	12	TFA/DE (1/3 vol/vol)	18 (0.84)	1.0
8TFA/DE	8	TFA/DE (1/3 vol/vol)	26 (0.26)	0.15
12HFIP	12	HFIP	18 (0.84)	1.5

above T_g, the nonwovens were placed between aluminum perforated plates, pressed, and held under the stress of approx. 5 kPa.

2.3. Characterization of nonwovens

The materials were examined with a scanning electron microscope (SEM) JEOL 6010LA (Japan) at an accelerating voltage of 10 kV. Before the examination, the surfaces were vacuum sputtered with 10 nm gold layers using a coater Quorum EMS150R ES (UK). The fiber diameter distributions were determined based on at least five SEM images of each nonwoven.

The surface densities of the nonwovens were determined based on their sizes and weight. The porosity was calculated according to the equation [50,51]:

$$Porosity = \left(1 - \frac{fibers\ volume}{nonwoven\ volume}\right) \cdot 100\ \% \tag{1}$$

assuming the density of amorphous PEF of 1.43 g/cm^3 [29].

The thermal stability and residual solvent content were determined by thermogravimetric analysis (TGA) using a TGA 5500 from TA Instruments (USA) during heating at 20 °C/min under nitrogen atmosphere.

The thermal properties were studied by differential scanning calorimetry (DSC), using a DSC3 from Mettler Toledo (Switzerland) during heating at 10 °C/min to 250 °C.

The water contact angles (WCA) of the nonwovens were determined by the drop method with 5 μL drops, at RT, using a 100-00-230 NRL Rame Hart goniometer (USA) and Image Drop Analysis program. In each case, the WCA measurements were carried out five times and average values were calculated. WCA was also measured for PEF film prepared by compression moulding at 250 °C.

Tensile drawing of nonwoven specimens was performed using a TST 350 Minitester from Linkam (UK) mounted in a polarized light microscope Nikon Eclipse 80i equipped with a Nikon DS-Fi1 video camera. At least three 10 mm wide strips of each material were gripped, with a distance between the grips of 20 mm, and drawn at 25 °C, at a rate of 2 mm/min (10%/min).

3. Results and discussion

TFA was chosen to dissolve PEF because it is a volatile polar solvent and it was used for electrospinning of other polymers, including PET [52,53]. In addition, electrospinning of PEF dissolved in mixtures of TFA with DM (TFA/DM, 1/3 vol/vol) and TFA with DE (TFA/DE, 1/3 vol/-vol), and in HFIP was explored. Preliminary experiments allowed to observe a general tendency of diminishing fiber diameter with decreasing polymer concentration, which had to be accompanied by the adjustment of the nozzle diameter and the flow rate. These results

permitted to find the electrospinning conditions suitable for the formation of a series of PEF nonwovens with defect-free fibers, with diameters in the nanometer and micrometer ranges. SEM micrographs of the nonwovens are collected in Figs. 1–4, whereas exemplary photographs are shown in Fig. S1 in Supporting Information (SI). Fig. S2 in SI presents fiber diameter distributions of the nonwovens additionally dried at 100 °C, whereas the corresponding average fiber diameters are plotted in Fig. 5 and listed in Table 2. It must be mentioned that the additional drying at 100 °C did not significantly affect the fiber diameter ranges, and increased markedly the average fiber diameters only in 6TFA and 8TFA nonwovens.

The PEF nonwovens obtained from its solutions in TFA consisted of exceptionally uniform, randomly oriented, smooth, and defect-free fibers, as shown in Fig. 1, with different diameters diminishing with decreasing PEF concentration. Additional SEM micrographs of the nonwovens are shown in Figs. S3 and S4 in SI. The diameters of most of 20TFA fibers were in the range of 2.0–2.4 μm, whereas the respective numbers for the other nonwovens were: 0.7–1.1 μm for 15TFA, 0.4–0.7 μm for 12TFA, 0.2–0.4 μm for 10TFA, 100–240 nm for 8TFA and 60–200 nm for 6TFA. The dependence of the average fiber diameter on the PEF concentration in solutions in TFA is presented in Fig. 5a. The electrospinning process from solutions in TFA with 12–20 wt% PEF concentration was carried at a dosing rate of 1.5 mL/h. The use of solutions in TFA with the lower PEF concentrations required the nozzles with smaller diameters and the lower dosing rates of 1.0 mL/h and 0.15 mL/h, as shown in Table 1.

The diameters of fibers obtained from PEF solutions in TFA/DM and TFA/DE mixtures depended on the second solvent, as shown in Fig. 5b and Table 2. The fibers electrospun from 12 wt% PEF solutions in TFA/DM and TFA/DE were thicker and thinner, respectively, than those in 12TFA obtained from the solution in TFA with the same PEF concentration, and their diameters were predominantly in the ranges of 0.6–1.4 μm and 0.2–0.45 μm, respectively. Also, 8TFA/DE fibers obtained from 8 wt% PEF solution in TFA/DE, with diameters in the range of 80–220 nm, were thinner than those of 8TFA. The thickest fibers were obtained from 12 wt% PEF solution in HFIP, with diameters ranging from 1.9 to 2.6 μm. These differences in fiber diameters can be explained considering the different evaporation rates of solvents during the motion of the polymer jets from the nozzle to the collector. It is worth noting that 12TFA/DM and 12HFIP fibers were obtained at the same dosing rate as 12TFA fibers, 1.5 mL/h, but reducing the rate to 1 mL/h and 0.15 mL/h was necessary in the case of electrospinning of 12TFA/DE and 8TFA/DE, respectively. SEM micrographs of the nonwovens electrospun from PEF solutions in TFA/DE and TFA/DM mixtures, and also in HFIP, are shown in Fig. 2. It must be mentioned that during electrospinning of 12TFA/DE the flow was less stable. That resulted in the formation of a small number of defects, in the form of local thickening of the fibers, as
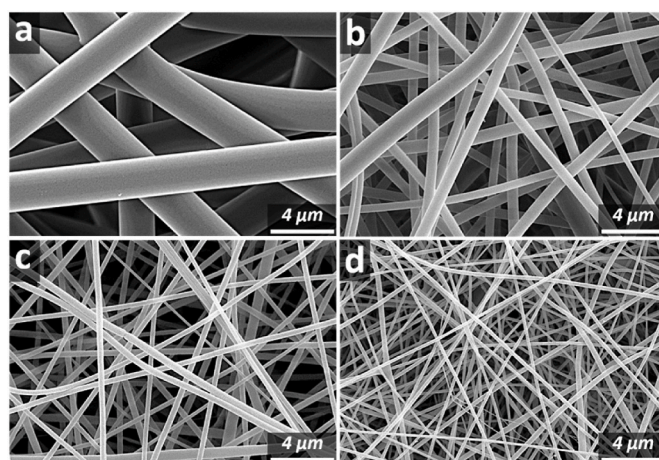

Fig. 2. SEM micrographs of PEF nonwovens electrospun from solutions in HFIP, and in TFA/DM and TFA/DE mixtures: a – 12HFIP, b – 12TFA/DM, c – 12TFA/DE, d – 8TFA/DE. Nonwovens dried at 60 °C.

illustrated in Fig. S5 (SI), due to too low viscosity of the solution. The fibers in the other nonwovens shown in Fig. 2 were smooth and defect-free.

The thinnest fibers were obtained from the solutions with the lowest PEF concentrations, 6 and 8 wt%. Due to such low polymer concentration, the reduction of the nozzle diameter and the dosing rate was necessary, as previously mentioned. The diameters of most of fibers in 8TFA and 6TFA were below 240 nm and 200 nm, respectively. 8TFA/DE fibers were thinner than those of 8TFA, with diameters below 220 nm. The processes of obtaining such thin fibers were very slow but resulted in smooth and defect-free fibers, as shown in Fig. 1e and f and Fig. 2d.

SEM micrographs of the nonwovens additionally dried at 100 °C are shown in Figs. 3 and 4. The micrographs evidence that the appearance of fibers did not change during drying.

The average fiber diameter, the nonwoven thickness, surface density and porosity calculated according to eq. (1) of the PEF nonwovens are collected in Table 2. It appears that drying at 100 °C did not affect significantly the average fiber diameters, except for the fibers in 6TFA and 8TFA, as it was already mentioned, but decreased the nonwoven thickness due to applied stress. The thickness of nonwovens dried at 60 °C ranged from 0.065 to 0.90 mm, but after drying at 100 °C it decreased to 0.035–0.33 mm. The thickest nonwovens were 20TFA and 15TFA, prepared from the solutions with high PEF concentration. In turn, the thinnest nonwovens were 8TFA, 6TFA and 8TFA/DE, with the thinnest fibers, obtained from the solutions with low PEF
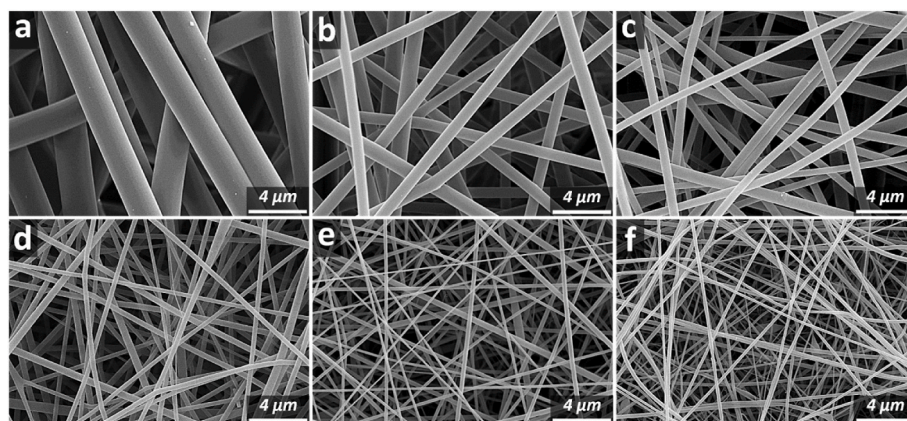

Fig. 1. SEM micrographs of nonwovens electrospun from PEF solutions in TFA: a – 20TFA, b – 15TFA, c – 12TFA, d – 10TFA, e – 8TFA, f – 6TFA. Nonwovens dried at 60 °C.
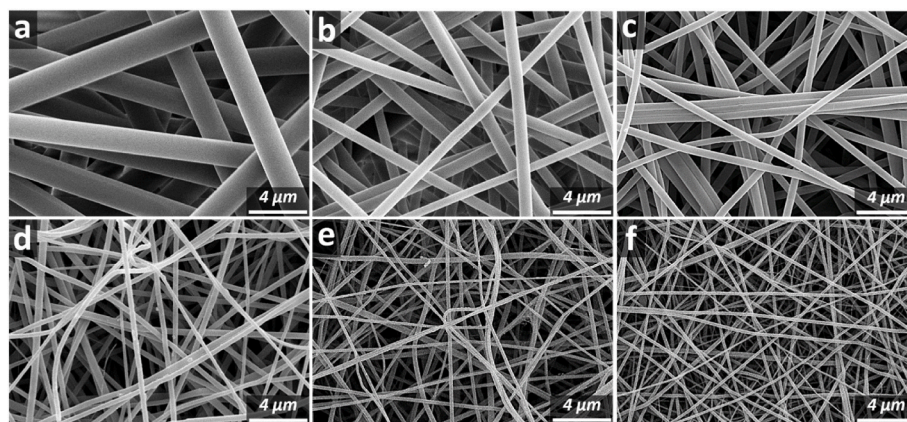
Fig. 3. SEM micrographs of nonwovens electrospun from PEF solutions in TFA: a – 20TFA, b – 15TFA, c – 12TFA, d – 10TFA, e – 8TFA, f – 6TFA. Nonwovens additionally dried at 100 °C.
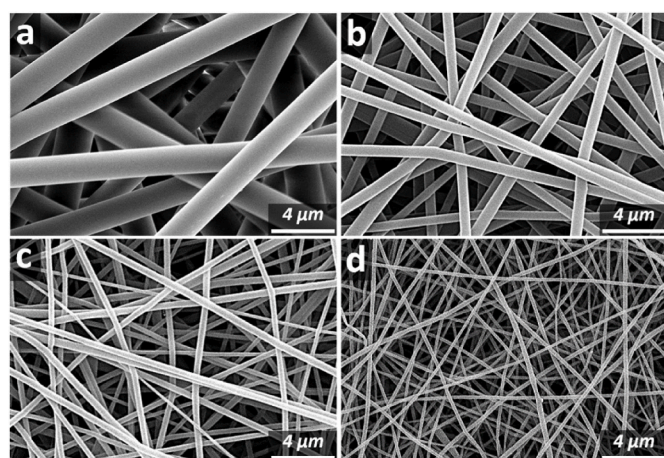

Fig. 4. SEM micrographs of PEF nonwovens electrospun from solutions in HFIP, and in TFA/DM and TFA/DE mixtures: a – 12HFIP, b – 12TFA/DM, c – 12TFA/DE, d – 8TFA/DE. Nonwovens additionally dried at 100 °C.

concentrations. The very small thickness of these nonwovens, below 0.1 mm, resulted from the reduced dosing rate, which made the process very slow, too slow to obtain thicker nonwovens within several hours. The surface density of the nonwovens dried at 60 °C was between 0.095 and 10.65 mg/cm^2 and decreased with their decreasing thickness. The porosity of all nonwovens dried at 60 °C was 90–92%, except for 12HFIP with a porosity of 86.5%. The surface density did not change significantly after drying at 100 °C and remained in the range of 0.84–12 mg/cm^2. Thus, the thickness decrease diminished the porosity to 74–88%. The decrease in porosity of the nonwovens with the thickest fibers, with

the exception of 12HFIP, was the strongest because of the strongest thickness reduction. The differences in the decrease in thickness were most possibly related to differences in stress transfer influenced by the nonwoven surface roughness, the fiber curvature, the porosity and the residual solvent content.

The barrier properties of PEF [12,15] inhibited the solvent evaporation during fiber formation and further drying. The TGA experiments evidenced the presence of residues of solvents in the fibers. TGA thermograms of PEF nonwovens, and also PEF granulate, recorded during heating from 25 to 350 °C at 20 °C/min in nitrogen atmosphere, are shown in Fig. S6 (SI), whereas the parameters determined from the thermograms are collected in Table 3. The weight loss of PEF granulate began around 350 °C and reached a peak rate at T_d of 419 °C. On the contrary, the weight loss of the nonwovens dried at 60 °C began above 60 °C and was obviously associated with the evaporation of solvents. The weight decrease of the nonwovens additionally dried at 100 °C started above 100 °C and was less pronounced. In most cases, the weight loss slowed down between 150 °C and 200 °C and significantly accelerated only above 300 °C due to PEF decomposition. Thus, the weight loss up to 200 °C (Δw_{200}) could serve as a measure of the residual solvent content. Among the nonwovens dried at 60 °C, 12HFIP, 20TFA, 15TFA and 12TFA/DE exhibited the largest Δw_{200} of 10.8, 7.3, 4.5 and 4.6 wt%, respectively, exceeding those of the other materials, 1.8–3.8 wt%. This is because of the diameters of 20TFA, 15TFA and 12HFIP fibers, exceeding the diameters of the other nonwoven fibers, the boiling point of DE above those of the other solvents used, and the relatively large molecule of HFIP, possibly impeding its diffusion in PEF. However, drying at 100 °C reduced significantly Δw_{200} in all cases, to 3.5 wt% for 12HFIP, and 0.2–0.6 wt% for the other nonwovens, except 8TFA and 6TFA.

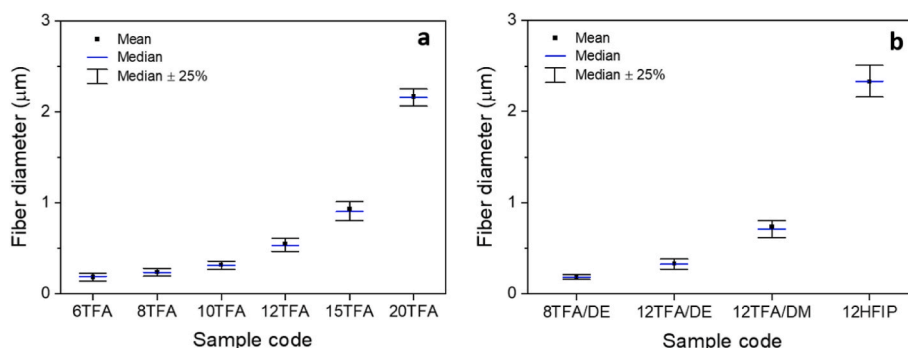T_d temperatures of the nonwovens dried at 60 °C, in the range of

Fig. 5. Fiber diameters in PEF nonwovens electrospun from solutions: a – in TFA, b – in TFA/DE, TFA/DM and HFIP.

Table 2
Characteristics of PEF nonwovens dried at 60 °C, and nonwovens additionally dried at 100 °C.

Sample code	Average fiber diameter (μm)		Thickness (mm)		Surface density (mg/cm^2)		Porosity (%)	
	60 °C	100 °C	60 °C	100 °C	60 °C	100 °C	60 °C	100 °C
20TFA	2.17	2.13	0.90	0.33	10.1	12.0	92	74
15TFA	0.92	0.93	0.90	0.29	10.6	10.5	92	75
12TFA	0.54	0.55	0.74	0.27	8.0	8.1	92	79
10TFA	0.31	0.32	0.64	0.22	7.6	5.7	92	82
8TFA	0.19	0.24	0.097	0.079	1.1	1.2	92	88
6TFA	0.13	0.18	0.099	0.066	1.1	1.2	92	87
12TFA/DM	0.79	0.74	0.45	0.28	6.1	5.7	91	86
12TFA/DE	0.33	0.33	0.39	0.15	4.9	4.6	91	79
8TFA/DE	0.16	0.18	0.065	0.035	0.95	0.84	90	85
12HFIP	2.24	2.33	0.33	0.25	6.4	6.0	86	83

Table 3
Thermogravimetric data of PEF nonwovens dried at 60 °C and nonwovens additionally dried at 100 °C: Δw_{200} – weight loss up to 200 °C; T_d – peak temperature of weight loss derivative with respect to temperature.

Sample code	Δw_{200} (%)		T_d (°C)	
	60 °C	100 °C	60 °C	100 °C
20TFA	7.3	0.3	408	410
15TFA	4.5	0.2	408	411
12TFA	3.1	0.2	411	413
10TFA	3.8	0.5	399	409
8TFA	3.0	1.5	403	407
6TFA	1.8	1.1	402	401
12TFA/DM	3.5	0.2	410	412
12TFA/DE	4.6	0.6	405	409
8TFA/DE	3.1	0.6	407	409
12HFIP	10.8	3.5	416	420
PEF granulate	0.05		419	

399–416 °C, were below that of PEF. After drying at 100 °C, T_d of 12HFIP increased to 420 °C. Although T_d temperatures of the other nonwovens increased to 401–413 °C, still were below that of PEF, indicating the adverse effect of the respective solvents on the thermal stability of the polymer. It is worth mentioning that the weight of 6TFA and 8TFA after the initial loss did not stabilize and continued to decrease, as shown in Fig. S6 (SI). There is no reason to expect that drying of these fibers was less effective than drying the other thicker fibers. Moreover, 6TFA and 8TFA exhibited the lowest T_d. Most probably a weight loss due to thermal decomposition of PEF began earlier in 6TFA and 8TFA than in the other materials and contributed to their Δw_{200}.

The TGA results showed that drying at 100 °C allowed to reduce significantly the residual solvent content, that remained in the fibers after the electrospinning process. It primarily depended on the solvent used. T_d temperatures of the nonwovens were below that of PEF, except for T_d of 12HFIP dried at 100 °C. In general, these temperatures were lower for the nonwovens dried at 60 °C than for those additionally dried at 100 °C with reduced residual solvent content, which indicates the adverse effect of the solvents on the thermal stability of the nonwovens. Nevertheless, as shown in Fig. S6 (SI) the nonwovens dried at 100 °C were stable up to 300 °C.

Exemplary DSC heating thermograms of the nonwovens dried at 60 °C, presented in Fig. S7 (SI), are featured by broad endotherms resulting from the solvent evaporation, which obscured the signal related to the thermal properties of PEF. The heating thermograms of the nonwovens additionally dried at 100 °C are plotted in Fig. 6, whereas the corresponding calorimetric parameters are collected in Table S1 (SI). The thermograms of nonwovens obtained from PEF solutions in TFA, TFA/DE and TFA/DM exhibited glass transitions, cold crystallization exotherms, and melting endotherms. T_g of these nonwovens was in the range of 85–87 °C. The sharp endotherms just above the glass transitions are related to the aging-induced enthalpy relaxation of the amorphous polymer [54,55]. The broad cold crystallization exotherms passed
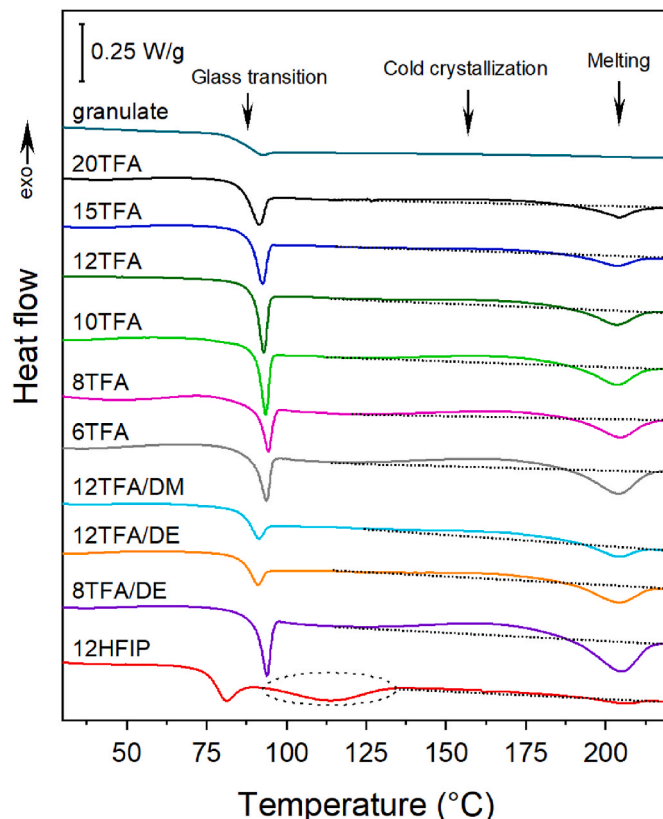

Fig. 6. First DSC heating thermograms of PEF nonwovens additionally dried at 100 °C, heating rate of 10 °C/min. The endotherm resulting from solvent evaporation from 12HFIP nonwoven marked with an ellipse. Thermogram of PEF granulate shown for comparison.

through maxima at T_{cc} of 164–168 °C and were followed by the melting endotherms with peak temperatures at 203–205 °C. The values of cold crystallization enthalpy (ΔH_{cc}) of 2.5–10.6 J/g were close to the values of melting enthalpy (ΔH_m), which indicates that the nonwovens were amorphous before heating in DSC. T_g of 12HFIP at 76 °C was below that of the other nonwovens because of the higher residual solvent content. The glass transition and enthalpy relaxation in 12HFIP were followed by the endotherm resulting from solvent evaporation. The cold crystallization exotherm and melting endotherm of 12HFIP were hardly visible with very small values of ΔH_{cc} and ΔH_m, close to 1 J/g. Fig. 6 shows also the heating thermogram of PEF granulate for comparison. The granulate was heated to 250 °C, after 5 min it was cooled to RT, heated to 100 °C, and annealed at 100 °C for 24 h. Above the glass transition with T_g at 86 °C neither cold crystallization nor melting were observed. This indicates that the weak cold crystallization in the fibers may be related to

the polymer chain orientation during electrospinning, more intense in the thinnest fibers, which could result in the formation of crystallization nuclei during further thermal treatment.

Water drops deposited on the nonwoven surfaces are shown in Fig. S8 (SI). All nonwovens were hydrophobic, unlike the PEF film with a WCA of 66°. The WCA values of the nonwovens dried at 60 °C were in the range of 153–155°, except for 20TFA and 15TFA with WCA of 164 and 159°, respectively. Others [56] found that nonwovens made of polymers, whose films exhibited WCA <90°, were hydrophobic with much higher WCA >90°. The reason was the surface roughness and air entrapped between fibers, which resulted in the Cassie-Baxter hydrophobicity regime. After additional drying at 100 °C, the WCA values of the nonwovens decreased to 144–146°, most possibly because of the decrease in surface roughness due to pressing during drying. However, the droplets placed on the nonwovens did not fall off but remained suspended when the mats were turned upside down, as illustrated in Fig. S9, due to the high adhesion of water to the fibers. The ability of certain rough surfaces to have a high WCA simultaneously with high adhesion to water is called 'the rose petal effect' [57,58]. Despite the high adhesion, the water did not soak into the nonwovens but remained in the form of stable droplets on their surfaces.

Fig. 7 shows exemplary engineering stress–engineering strain dependencies of the PEF nonwovens, whereas the average values of mechanical parameters are collected in Table 4. The PEF electrospun nonwovens had a loose structure with randomly oriented fibers. The loosely connected structure without strong bonds between the fibers at their cross points facilitated changes in the fiber arrangement during stretching. When the stretching started, fibers with their ends held by grips began to align in the stretching direction. Those that were not clamped were rather pulled apart and remained less oriented in the stretching direction, as illustrated in Fig. S10 (SI).

The nonwovens dried at 60 °C exhibited the tensile strength of 2.3–3.7 MPa, and the elongation at break of 40–145%. The elongation at break of the nonwovens additionally dried at 100 °C ranged from 52 to 190%. Moreover, drying at 100 °C increased the strength to 5.3–10.8 MPa.

It is worth noting that the tensile strength of 1–2.7 MPa and the elongation at break of 180–480% were reported for PET nonwovens with average fiber diameter in the range of 0.7–1.2 μm, drawn at a rate of 2.5%/min [59]. In turn, the PET nonwoven with an average fiber diameter of 1.7 μm, drawn at a rate of 20%/min, exhibited the tensile strength of 0.94 MPa and the elongation at break near 47% [60].

The stress in Fig. 7 and the tensile strength of nonwovens in Table 4 were calculated by dividing the force by the nonwoven cross-section area, thus the decrease in nonwoven thickness due to drying at 100 °C improved the calculated tensile strength. However, the improvement of the strength of 20TFA, 15TFA and 12TFA was greater than the increase that could be anticipated based on the reduction of their thicknesses. We hypothesize that the diminishing residual solvent content and the

Table 4
Mechanical parameters (average values) of PEF nonwovens additionally dried at 100 °C.

Sample code	Tensile strength of nonwovens (MPa)	Tensile strength of fibers (MPa)	Elongation at break (%)
20TFA	10.8	41.5	190
15TFA	8.6	34.4	76
12TFA	7.9	37.6	150
10TFA	5.3	29.4	52
12TFA/ DM	5.6	40.0	150
12TFA/ DE	6.7	31.9	71
12HFIP	5.9	31.2	87

enhancement of bonding between the fibers due to pressing could contribute to the strength increase. However, it should be noted that the annealing above T_g could also result in relaxation of the polymer chain orientation and adversely affect the strength of the fibers. As can be seen in Fig. 7, in almost all cases the strength was determined by the stress at break, which exceeded the yield stress. The only exception was 12HFIP, for which the stress at break was lower than the yield stress, hence the latter was taken as the tensile strength. Although 12HFIP contained thick fibers with an average diameter of 2.33 μm, its strength was low due to the plasticizing effect of the solvent residue, which was also reflected in the low T_g of this material. It is obvious that the porosity of nonwovens is an important factor influencing their tensile behavior because only fibers can bear the load. The tensile strength of fibers, calculated by dividing the maximum force by the fraction of the nonwoven cross-section occupied by the fibers, was in the range of 32.2–41.5 MPa, as shown in Table 4. The elimination of the effect of porosity diminished the differences between the materials. The strength of fibers, listed in Table 4, showed a downward trend with the decreasing average fiber diameter. The highest strength was that of 20TFA, with an average fiber diameter of 2.13 μm, whereas the other nonwovens, with thinner fibers, exhibited lower strength. It also appears that the highest values of elongation at break correlated with the highest strength of the fibers. It is worth noting that the tensile strength of PEF films close to 40 MPa was previously measured by others [11], although the higher value of 67 MPa was also reported [9].

4. Conclusions

A series of novel bio-based PEF nonwovens was obtained by solution electrospinning and examined for the first time. Smooth and defect-free fibers with uniform diameters were obtained. The average diameters of fibers electrospun from PEF solutions in TFA, and in TFA/DE and TFA/DM mixtures, after drying ranged from 2.13 μm to 180 nm, depending on the solvent type and decreased with decreasing PEF concentration in the solutions, from 20 to 6 wt%. The fibers obtained from PEF solutions
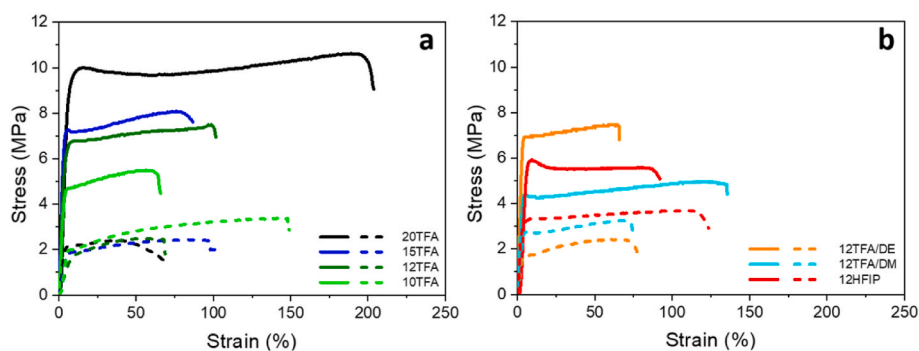

Fig. 7. Exemplary stress-strain dependencies of PEF nonwovens electrospun from solutions: a –in TFA, b – in HFIP, TFA/DM and TFA/DE mixtures. Dashed lines – nonwovens dried at 60 °C, solid lines – nonwovens additionally dried at 100 °C.

in TFA/DM and TFA/DE mixtures were thicker and thinner, respectively, than those obtained from PEF solutions in TFA alone, with the same polymer concentration. Drying under reduced pressure at 60 °C for 24 h did not sufficiently reduce the residual solvent content in the fibers. To achieve this aim, additional drying at 100 °C for 24 h was necessary. The dried fibers were amorphous with T_g at 85–87 °C, and remained straight, uniform, and defect-free. 12HFIP fibers, obtained from PEF solution in HFIP, were thicker than 12TFA fibers obtained from PEF solution in TFA, and after drying still contained about 3.5 wt% of the solvent, which decreased their T_g to 76 °C. The dried nonwovens were strongly hydrophobic with WCA angles of 144–146°, although they exhibited the rose petal effect. The mechanical properties of the dried nonwovens were influenced primarily by their porosity and fiber thickness, although in the case of 12HFIP nonwoven the plasticizing effect of HFIP residue was observed. The dried nonwovens exhibited the tensile strength from 5.3 to 10.8 MPa, and the elongation at break from 52 to 190%. The highest values of both parameters were measured for 20TFA nonwoven obtained from 20 wt% PEF solution in TFA, with an average fiber diameter of 2.13 μm.

Author statement

Mariia Svyntkivska: Conceptualization, Methodology, Investigation, Analysis of results, Writing – original draft; **Tomasz Makowski:** Conceptualization, Methodology, Writing – review and editing; **Ele L. de Boer:** Conceptualization, Writing – review and editing; **Ewa Piorkowska:** Conceptualization, Supervision, Writing – review and editing.

Declaration of competing interest

The authors declare that they have no known competing financial interests or personal relationships that could have appeared to influence the work reported in this paper.

Acknowledgments

Appendix A. Supplementary data

Supplementary data to this article can be found online at https://doi.org/10.1016/j.polymertesting.2022.107677.

References

[1] J.G. Rosenboom, D.K. Hohl, P. Fleckenstein, G. Storti, M. Morbidelli, Bottle-grade polyethylene furanoate from ring-opening polymerisation of cyclic oligomers, Nat. Commun. 9 (2018) 2701, https://doi.org/10.1038/s41467-018-05147-y.

[2] N. Guigo, E. Forestier, N. Sbirrazzuoli, Thermal properties of biobased polymers: furandicarboxylic acid (FDCA)-Based polyesters, Adv. Polym. Sci. 283 (2019) 189–217, https://doi.org/10.1007/12_2019_51.

[3] Global Polyethylene Furanoate Market 2018-2025 - Ongoing Quest to Decrease the Global Carbon Footprint Is a Major Driver, 24 January 2022. https://www.prnewswire.com/news-releases/global-polyethylene-furanoate-market-2018-2025—ongoing-quest-to-decrease-the-global-carbon-footprint-is-a-major-driver-300689405.html.

[4] PEF – the Polymer for the Future, 24 January 2022 access, https://www.avantium.com/publication/pef-the-polymer-for-the-future/.

[5] X. Fei, J.G. Wang, J. Zhu, X.Z. Wang, X.Q. Liu, Biobased poly(ethylene 2,5-furancoate): No longer an alternative, but an irreplaceable polyester in the polymer industry, ACS Sustain. Chem. Eng. 8 (2020) 8471–8485, https://doi.org/10.1021/acssuschemeng.0c01862.

[6] W.H. Faveere, S. Van Praet, B. Vermeeren, K.N.R. Dumoleijn, K. Moonen, E. Taarning, B.F. Sels, Toward replacing ethylene oxide in a sustainable world: glycolaldehyde as a bio-based C-2 platform molecule, Angew. Chem. Int. Ed. 60 (2021) 12204–12223, https://doi.org/10.1002/anie.202009811.

[7] M.B. Banella, J. Bonucci, M. Vannini, P. Marchese, C. Lorenzetti, A. Celli, Insights into the synthesis of poly(ethylene 2,5-furandicarboxylate) from 2,5-furandicarboxylic acid: steps toward environmental and food safety excellence in packaging applications, Ind. Eng. Chem. Res. 58 (2019) 8955–8962, https://doi.org/10.1021/acs.iecr.9b00661.

[8] J.J. Kolstad, G.J.M. Gruter, Process for the Preparation of a Fiber, a Fiber and a Yarn Made from Such a Fiber, EP 3011086 B1, 2018.

[9] M. Jiang, Q. Liu, Q. Zhang, C. Ye, G.Y. Zhou, A series of furan-aromatic polyesters synthesized via direct esterification method based on renewable resources, J. Polym. Sci.: Polym. Chem. 50 (2012) 1026–1036, https://doi.org/10.1002/pola.25859.

[10] J.G. van Berkel, N. Guigo, J.J. Kolstad, L. Sipos, B. Wang, M.A. Dam, N. Sbirrazzuoli, Isothermal crystallization kinetics of poly (ethylene 2,5-furandicarboxylate), Macromol. Mater. Eng. 300 (2015) 466–474, https://doi.org/10.1002/mame.201400376.

[11] R.J.I. Knoop, W. Vogelzang, J. van Haveren, D.S. van Es, High molecular weight poly(ethylene-2,5-furanoate); critical aspects in synthesis and mechanical property determination, J. Polym. Sci.: Polym. Chem. 51 (2013) 4191–4199, https://doi.org/10.1002/pola.26833.

[12] S.K. Burgess, O. Karvan, J.R. Johnson, R.M. Kriegel, W.J. Koros, Oxygen sorption and transport in amorphous poly(ethylene furanoate), Polymer 55 (2014) 4748–4756, https://doi.org/10.1016/j.polymer.2014.07.041.

[13] S.K. Burgess, D.S. Mikkilineni, D.B. Yu, D.J. Kim, C.R. Mubarak, R.M. Kriegel, W.J. Koros, Water sorption in poly(ethylene furanoate) compared to poly(ethylene terephthalate). Part 2: kinetic sorption, Polymer 55 (2014) 6870–6882, https://doi.org/10.1016/j.polymer.2014.10.065.

[14] S.K. Burgess, D.S. Mikkilineni, D.B. Yu, D.J. Kim, C.R. Mubarak, R.M. Kriegel, W.J. Koros, Water sorption in poly(ethylene furanoate) compared to poly(ethylene terephthalate). Part 1: equilibrium sorption, Polymer 55 (2014) 6861–6869, https://doi.org/10.1016/j.polymer.2014.10.047.

[15] S.K. Burgess, R.M. Kriegel, W.J. Koros, Carbon dioxide sorption and transport in amorphous poly(ethylene furanoate), Macromolecules 48 (2015) 2184–2193, https://doi.org/10.1021/acs.macromol.5b00333.

[16] S.K. Burgess, G.B. Wenz, R.M. Kriegel, W.J. Koros, Penetrant transport in semicrystalline poly(ethylene furanoate), Polymer 98 (2016) 305–310, https://doi.org/10.1016/j.polymer.2016.06.046.

[17] L.Y. Sun, J.G. Wang, S. Mahmud, Y.H. Jiang, J. Zhu, X.Q. Liu, New insight into the mechanism for the excellent gas properties of poly (ethylene 2,5-furandicarboxylate) (PEF): role of furan ring's polarity, Eur. Polym. J. 118 (2019) 642–650, https://doi.org/10.1016/j.eurpolymj.2019.06.033.

[18] Z. Terzopoulou, L. Papadopoulos, A. Zamboulis, D.G. Papageorgiou, G. Z. Papageorgiou, D.N. Bikiaris, Tuning the properties of furandicarboxylic acid-based polyesters with copolymerization: a review, Polymers 12 (2020) 1209, https://doi.org/10.3390/polym12061209.

[19] P. Wang, W. Huang, Y.J. Zhang, J.Y. Lin, P. Chen, An evoluted bio-based 2,5-furandicarboxylate copolyester fiber from poly(ethylene terephthalate), J. Polym. Sci. 58 (2020) 320–329, https://doi.org/10.1002/pol.20190057.

[20] H.Z. Xie, L.B. Wu, B.G. Li, P. Dubois, Modification of poly(ethylene 2,5-furandicarboxylate) with biobased 1,5-pentanediol: significantly toughened copolyesters retaining high tensile strength and O-2 barrier property, Biomacromolecules 20 (2019) 353–364, https://doi.org/10.1021/acs.biomac.8b01495.

[21] J.G. Wang, X.Q. Liu, Y.J. Zhang, F. Liu, J. Zhu, Modification of poly(ethylene 2,5-furandicarboxylate) with 1,4-cyclohexanedimethylene: influence of composition on mechanical and barrier properties, Polymer 103 (2016) 1–8, https://doi.org/10.1016/j.polymer.2016.09.030.

[22] J. Wang, S. Mahmud, X. Zhang, J. Zhu, Z. Shen, X. Liu, Biobased amorphous polyesters with high Tg: trade-off between rigid and flexible cyclic diols, ACS Sustain. Chem. Eng. 7 (2019) 6401–6411, https://doi.org/10.1021/acssuschemeng.9b00285.

[23] A. Codou, N. Guigo, J.G. van Berkel, E. de Jong, N. Sbirrazzuoli, Preparation and characterization of poly(ethylene 2,5-furandicarboxylate/nanocrystalline cellulose composites via solvent casting, J. Polym. Eng. 37 (2017) 869–878, https://doi.org/10.1515/polyeng-2017-0042.

[24] A. Codou, N. Guigo, J.G. van Berkel, E. de Jong, N. Sbirrazzuoli, Preparation and crystallization behavior of poly(ethylene 2,5-furandicarboxylate)/cellulose composites by twin screw extrusion, Carbohydr. Polym. 174 (2017) 1026–1033, https://doi.org/10.1016/j.carbpol.2017.07.006.

[25] L. Martino, N. Guigo, J.G. van Berkel, N. Sbirrazzuoli, Influence of organically modified montmorillonite and sepiolite clays on the physical properties of bio-based poly(ethylene 2,5-furandicarboxylate), Compos. B Eng. 110 (2017) 96–105, https://doi.org/10.1016/j.compositesb.2016.11.008.

[26] A. Koltsakidou, Z. Terzopoulou, G.Z. Kyzas, D.N. Bikiaris, D.A. Lambropoulou, Biobased poly(ethylene furanoate) polyester/TiO2 supported nanocomposites as effective photocatalysts for anti-inflammatory/analgesic drugs, Molecules 24 (2019) 564, https://doi.org/10.3390/molecules24030564.

[27] N. Poulopoulou, A. Pipertzis, N. Kasmi, D.N. Bikiaris, D.G. Papageorgiou, G. Floudas, G.Z. Papageorgiou, Green polymeric materials: on the dynamic homogeneity and miscibility of furan-based polyester blends, Polymer 174 (2019) 187–199, https://doi.org/10.1016/j.polymer.2019.04.058.

[28] A. Gandini, D. Coelho, M. Gomes, B. Reis, A. Silvestre, Materials from renewable resources based on furan monomers and furan chemistry: work in progress, J. Mater. Chem. 19 (2009) 8656–8664, https://doi.org/10.1039/b909377j.

[29] S.K. Burgess, J.E. Leisen, B.E. Kraftschik, C.R. Mubarak, R.M. Kriegel, W.J. Koros, Chain mobility, thermal, and mechanical properties of poly(ethylene furanoate)

compared to poly(ethylene terephthalate), Macromolecules 47 (2014) 1383–1391, https://doi.org/10.1021/ma5000199.

[30] J.G. van Berkel, N. Guigo, H.A. Visser, N. Sbirrazzuoli, Chain structure and molecular weight dependent mechanics of poly(ethylene 2,5-furandicarboxylate) compared to poly(ethylene terephthalate), Macromolecules 51 (2018) 8539–8549, https://doi.org/10.1021/acs.macromol.8b01831.

[31] A. Codou, N. Guigo, J. van Berkel, E. de Jong, N. Sbirrazzuoli, Non-isothermal crystallization kinetics of biobased poly(ethylene 2,5-furandicarboxylate) synthesized via the direct esterification process, Macromol. Chem. Phys. 215 (2014) 2065–2074, https://doi.org/10.1002/macp.201400316.

[32] C. Menager, N. Guigo, L. Martino, N. Sbirrazzuoli, H. Visser, S.A.E. Boyer, N. Billon, G. Monge, C. Combeaud, Strain induced crystallization in biobased Poly (ethylene 2,5-furandicarboxylate) (PEF); conditions for appearance and microstructure analysis, Polymer 158 (2018) 364–371, https://doi.org/10.1016/j.polymer.2018.10.054.

[33] T. Hohnemann, M. Steinmann, S. Schindler, M. Hoss, S. Konig, A. Ota, M. Dauner, M.R. Buchmeiser, Poly(Ethylene furanoate) along its life-cycle from a polycondensation approach to high-performance yarn and its recyclate, Materials 14 (2021) 1044, https://doi.org/10.3390/ma14041044.

[34] W. Takarada, K. Sugimoto, H. Nakajima, H.A. Visser, G.J.M. Gruter, T. Kikutani, Melt-spun fibers from bio-based polyester-fiber structure development in high-speed melt spinning of poly(ethylene 2,5-furandicarboxylate) (PEF), Materials 14 (2021) 1172, https://doi.org/10.3390/ma14051172.

[35] P. Ji, D.P. Lu, S.M. Zhang, W.Y. Zhang, C.S. Wang, H.P. Wang, Modification of poly (ethylene 2,5-furandicarboxylate) with poly(ethylene glycol) for biodegradable copolyesters with good mechanical properties and spinnability, Polymers 11 (2019) 2105, https://doi.org/10.3390/polym11122105.

[36] D. Rigotti, G. Fredi, D. Perin, D.N. Bikiaris, A. Pegoretti, A. Dorigato, Statistical modeling and optimization of the drawing process of bioderived polylactide/poly (dodecylene furanoate) wet-spun fibers, Polymers 14 (2022) 396, https://doi.org/10.3390/polym14030396.

[37] D. Perin, D. Rigotti, G. Fredi, G.Z. Papageorgiou, D.N. Bikiaris, A. Dorigato, Innovative bio-based poly(lactic acid)/poly(alkylene Furanoate)s fiber blends for sustainable textile applications, J. Polym. Environ. 29 (2021) 3948–3963, https://doi.org/10.1007/s10924-021-02161-y.

[38] Y. Liao, C.H. Loh, M. Tian, R. Wang, A.G. Fane, Progress in electrospun polymeric nanofibrous membranes for water treatment: fabrication, modification and applications, Prog. Polym. Sci. 77 (2018) 69–94, https://doi.org/10.1016/j.progpolymsci.2017.10.003.

[39] Y.J. Ryu, H.Y. Kim, K.H. Lee, H.C. Park, D.R. Lee, Transport properties of electrospun nylon 6 nonwoven mats, Eur. Polym. J. 39 (2003) 1883–1889, https://doi.org/10.1016/s0014-3057(03)00096-x.

[40] J.X. Ding, J. Zhang, J.N. Li, D. Li, C.S. Xiao, H.H. Xiao, H.H. Yang, X.L. Zhuang, X. S. Chen, Electrospun polymer biomaterials, Prog. Polym. Sci. 90 (2019) 1–34, https://doi.org/10.1016/j.progpolymsci.2019.01.002.

[41] J.J. Xue, T. Wu, Y.Q. Dai, Y.N. Xia, Electrospinning and electrospun nanofibers: methods, materials, and applications, Chem. Rev. 119 (2019) 5298–5415, https://doi.org/10.1021/acs.chemrev.8b00593.

[42] J.C. Ge, J.Y. Kim, S.K. Yoon, N.J. Choi, Fabrication of low-cost and high-performance coal fly ash nanofibrous membranes via electrospinning for the control of harmful substances, Fuel 237 (2019) 236–244, https://doi.org/10.1016/j.fuel.2018.09.068.

[43] X. Qin, S. Subianto, Electrospun nanofibers for filtration applications, in: M. Afshari (Ed.), Electrospun Nanofibers, Woodhead Publishing, 2017, pp. 449–466.

[44] Z.M. Zhang, Z.Q. Gan, R.Y. Bao, K. Ke, Z.Y. Liu, M.B. Yang, W. Yang, Green and robust superhydrophilic electrospun stereocomplex polylactide membranes:

[45] multifunctional oil/water separation and self-cleaning, J. Membr. Sci. 593 (2020), 117420, https://doi.org/10.1016/j.memsci.2019.117420.

[45] S. Ataei, P. Azari, A. Hassan, B. Pingguan-Murphy, R. Yahya, F. Muhamad, Essential oils-loaded electrospun biopolymers: a future perspective for active food packaging, Adv. Polym. Technol. 2020 (2020), 9040535, https://doi.org/10.1155/2020/9040535.

[46] L.Y. Zhao, G.G. Duan, G.Y. Zhang, H.Q. Yang, S.J. He, S.H. Jiang, Electrospun functional materials toward food packaging applications: a review, Nanomaterials 10 (2020) 150, https://doi.org/10.3390/nano10010150.

[47] H.S. Sofi, A. Abdal-hay, S. Ivanovski, Y.S. Zhang, F.A. Sheikh, Electrospun nanofibers for the delivery of active drugs through nasal, oral and vaginal mucosa: current status and future perspectives, Mater. Sci. Eng. C 111 (2020), 110756, https://doi.org/10.1016/j.msec.2020.110756.

[48] X.Q. Tong, W.H. Pan, T. Su, M.Y. Zhang, W. Dong, X.L. Qi, Recent advances in natural polymer-based drug delivery systems, React. Funct. Polym. 148 (2020), 104501, https://doi.org/10.1016/j.reactfunctpolym.2020.104501.

[49] B. Kost, M. Svyntkivska, M. Brzezinski, T. Makowski, E. Piorkowska, K. Rajkowska, A. Kunicka-Styczynska, T. Biela, PLA/beta-CD-based fibres loaded with quercetin as potential antibacterial dressing materials, Colloids Surf., B 190 (2020), 9040535, https://doi.org/10.1016/j.colsurfb.2020.110949.

[50] M.M. Kareem, K.E. Tanner, Optimising micro-hydroxyapatite reinforced poly (lactide acid) electrospun scaffolds for bone tissue engineering, J. Mater. Sci. Mater. Med. 31 (2020) 38, https://doi.org/10.1007/s10856-020-06376-8.

[51] M.K. Selatile, S.S. Ray, V. Ojijo, R. Sadiku, Correlations between fibre diameter, physical parameters, and the mechanical properties of randomly oriented biobased polylactide nanofibres, Fibers Polym. 20 (2019) 100–112, https://doi.org/10.1007/s12221-019-8262-z.

[52] B. Veleirinho, M.F. Rei, J.A. Lopes-da-Silva, Solvent and concentration effects on the properties of electrospun poly(ethylene terephthalate) nanofiber mats, J. Polym. Sci. B Polym. Phys. 46 (2008) 460–471, https://doi.org/10.1002/polb.21380.

[53] S. Jafari, S.S.H. Salekdeh, A. Solouk, M. Yousefzadeh, Electrospun polyethylene terephthalate (PET) nanofibrous conduit for biomedical application, Polym. Adv. Technol. 31 (2020) 284–296, https://doi.org/10.1002/pat.4768.

[54] J.M. Hutchinson, Physical aging of polymers, Prog. Polym. Sci. 20 (1995) 703–760, https://doi.org/10.1016/0079-6700(94)00001-I.

[55] K. Abbès, G. Vigier, J.Y. Cavaillé, L. David, A. Faivre, J. Perez, Isoconfigurational state dependent molecular mobility in the glass temperature range, J. Non-Cryst. Solids 235–237 (1998) 286–292, https://doi.org/10.1016/S0022-3093(98)00590-0.

[56] P.K. Szewczyk, D.P. Ura, S. Metwally, J. Knapczyk-Korczak, M. Gajek, M. M. Marzec, A. Bernasik, U. Stachewicz, Roughness and fiber fraction dominated wetting of electrospun fiber-based porous meshes, Polymers 11 (2019) 34, https://doi.org/10.3390/polym11010034.

[57] B. Bhushan, M. Nosonovsky, Rose petal effect, in: B. Bhushan (Ed.), Encyclopedia of Nanotechnology, Springer Netherlands, Dordrecht, 2012, pp. 2265–2272.

[58] Z.H. Pan, F.Q. Cheng, B.X. Zhao, Bio-inspired polymeric structures with special wettability and their applications: an overview, Polymers 9 (2017) 725, https://doi.org/10.3390/polym9120725.

[59] K.W. Kim, K.H. Lee, M.S. Khil, Y.S. Ho, H.Y. Kim, The effect of molecular weight and the linear velocity of drum surface on the properties of electrospun poly (ethylene terephthalate) nonwovens, Fibers Polym. 5 (2004) 122–127, https://doi.org/10.1007/bf02902925.

[60] L.N. Wang, C.Z. Xin, W.T. Liu, X.L. Xia, S.Q. He, H. Liu, C.S. Zhu, Electrospun PET/PEG fibrous membrane with enhanced mechanical properties and hydrophilicity for filtration applications, Arabian J. Sci. Eng. 40 (2015) 2889–2895, https://doi.org/10.1007/s13369-015-1828-1.

Update

Polymer Testing
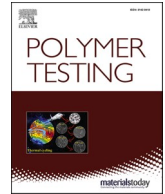
Corrigendum to "Solution electrospinning and properties of poly(ethylene 2,5-furandicarboxylate) fibers" [Polym. Test. 113 (2022) 107677]

Mariia Svyntkivska [a,*], Tomasz Makowski [a], Ele L. de Boer [b], Ewa Piorkowska [a]

[a] Centre of Molecular and Macromolecular Studies Polish Academy of Sciences, Sienkiewicza 112, 90-363, Lodz, Poland
[b] Avantium Renewable Polymers BV, Zekeringstraat 29, 1014 BV, Amsterdam, the Netherlands

The authors regret that there were errors in the Result and Discussion section. In the text below Table 3 T_d temperatures of the nonwovens were compared to that of PEF granulate. Hence, in the text, 'PEF' should be replaced with 'PEF granulate'. Moreover, the description of Table 3 should contain information on the drying of the PEF granulate.

The correct text is shown below:

Table 3
Thermogravimetric data of PEF nonwovens dried at 60 °C and nonwovens additionally dried at 100 °C: Δw_{200} – weight loss up to 200 °C, T_d – peak temperature of weight loss derivative with respect to temperature. PEF granulate was dried at 140 °C for 16 h.

T_d temperatures of the nonwovens dried at 60 °C, in the range of 399–416 °C, were below that of PEF granulate. After drying at 100 °C, T_d of 12HFIP increased to 420 °C. Although T_d temperatures of the other nonwovens increased to 401–413 °C, still were below that of PEF granulate, indicating the adverse effect of the respective solvents on the thermal stability of the polymer. It is worth mentioning that the weight of 6TFA and 8TFA after the initial loss did not stabilize and continued to decrease, as shown in Fig. S6 (SI). There is no reason to expect that drying of these fibers was less effective than drying the other thicker fibers. Moreover, 6TFA and 8TFA exhibited the lowest T_d. Most probably a weight loss due to thermal decomposition of PEF began earlier in 6TFA and 8TFA than in the other materials and contributed to their Δw_{200}.

The TGA results showed that drying at 100 °C allowed to reduce significantly the residual solvent content, that remained in the fibers after the electrospinning process. It primarily depended on the solvent used. T_d temperatures of the nonwovens were below that of PEF granulate, except for T_d of 12HFIP dried at 100 °C.

The authors would like to apologise for any inconvenience caused.